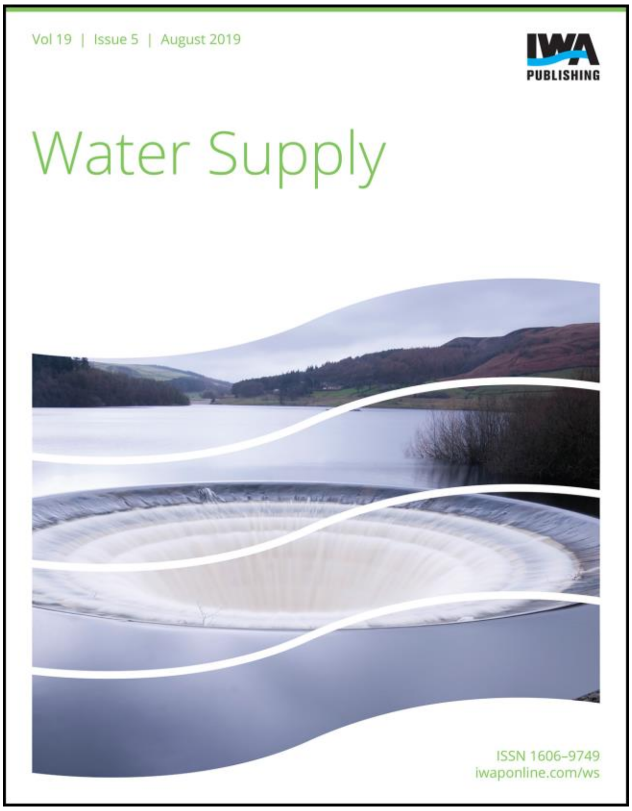
Vol 19 | Issue 5 | August 2019
IWA
PUBLISHING
Water Supply
ISSN 1606-9749
iwaponline.com/ws

Water Supply | 19.5 | 2019

Spatial variability and temporal dynamics of cyanobacteria blooms and water quality parameters in Missisquoi Bay (Lake Champlain)

I. Melendez-Pastor, E. M. Isenstein, J. Navarro-Pedreño and M-H. Park

ABSTRACT

Cyanobacteria bloom events have been associated with eutrophication processes, along with hydrologic and climate factors. Missisquoi Bay is a portion of Lake Champlain (USA–Canada) that is highly eutrophic and prone to cyanobacteria blooms and cyanotoxins. This study assessed the spatial–temporal influence of nutrients, turbidity and temperature in cyanobacteria distributions during a bloom event in the summer of 2006. Correlations, generalized linear models (GLMs), geostatistics and local indications of spatial association (LISA) autocorrelation analysis tested the influence of nutrient and non-nutrient explanatory variables in cyanobacteria biovolume. Total phosphorus exhibited a high direct correlation with cyanobacteria biovolume. The best performing GLMs included total phosphorus, total nitrogen, Secchi depth (as turbidity) and temperature as explanatory variables of cyanobacteria biovolume. Variogram analysis of those variables resulted in a better understanding of the underlying spatial variation process of the cyanobacteria bloom event. The LISA test revealed a moderate but stable autocorrelation between cyanobacteria biovolume and total phosphorus from 180 to 1,000 m of weight distance, suggesting the possibility of up-scaling the current results to coarse-resolution satellite imagery for more frequent monitoring of bloom events. The LISA test also revealed the spatial–temporal dynamic (movement of cyanobacteria scums) of high cyanobacteria blooms with high total phosphorus concentration.

Key words | autocorrelation, cyanobacteria, harmful algal bloom, Lake Champlain, remote sensing

I. Melendez-Pastor (corresponding author)
J. Navarro-Pedreño
Department of Agrochemistry and Environment,
University Miguel Hernandez (UMH),
Av/ Universidad s/n, Edificio Alcudia, 03202 Elche,
Spain
E-mail: *imelendez@umh.es*

E. M. Isenstein
Department of Civil and Environmental Engineering,
University of Massachusetts Amherst (UMASS),
130 Natural Resources Road, Amherst, Massachusetts 01003,
USA

M-H. Park
Department of Civil and Environmental Engineering,
University of California,
Los Angeles,
USA

INTRODUCTION

Cyanobacteria harmful algal blooms (CyanoHABs) are a serious problem in many freshwater and seawater ecosystems. Mass development of cyanobacteria has severe impacts on aquatic ecosystems such as: (1) increasing the turbidity of eutrophied water bodies, thus suppressing the establishment and growth of aquatic macrophytes; (2) depleting night-time oxygen; (3) causing odor problems; and (4) producing toxins that threaten water usage (Paerl & Huisman 2009).

Many research efforts have been focused on the identification and analysis of the driving factors leading to the development of CyanoHABs to promote prevention and mitigation strategies. Nutrients and hydrology are identified as the most common factors that promote CyanoHABs (Paerl 2008). A strong relationship between cyanobacteria concentrations and major nutrients (i.e. nitrogen and phosphorus) has been extensively reported (Anderson *et al.* 2002). Additionally, nutrient inputs may interact with hydrological features such as sedimentation, freshwater discharge and water column stability (Paerl 2008). Climate also plays a major role in controlling CyanoHABs as their dominance is promoted with increased temperatures, atmospheric CO_2 supplies and more intense precipitation events (Paerl & Huisman 2009; Paerl *et al.* 2011a).

doi: 10.2166/ws.2019.017

The distribution of CyanoHABs during bloom episodes has complex spatial and temporal variations (Agha *et al.* 2012). The patchiness of cyanobacterial blooms is not observed using conventional monitoring programs (Kutser *et al.* 2006). Remote sensing is useful for monitoring CyanoHABs and has been applied to inland waters (Matthews *et al.* 2010; Wheeler *et al.* 2012; Isenstein & Park 2014).

This study assessed the influence of nutrients, turbidity and temperature on CyanoHAB distribution in a lake system during bloom events. The objectives of this study are: (1) to establish the spatial–temporal relation among cyanobacteria and selected environmental variables obtained from satellite imagery (i.e., Landsat); and (2) to assess the spatial autocorrelation among cyanobacteria and the environmental variables at multiple resolutions.

MATERIALS AND METHODS

The study area focuses on Missisquoi Bay (Canada–USA border), which is located in the northeast of Lake Champlain (Figure S-1, available with the online version of this paper). The Bay is shallow water (up to 5 m of depth) with a limited water flux to the rest of the lake. Major water inputs into the Bay are the Missisquoi River that flows from the south and the Pike River that flows from the north. Paleolimnological studies have evidenced that Missisquoi Bay remained mesotrophic until agriculture intensified after 1970 (Levine *et al.* 2012), and thereafter the Bay became highly eutrophic with high phosphorus inputs and prone to expansive cyanobacteria blooms during the summer (Boyer 2008; Bowling *et al.* 2015).

The distributions of cyanobacteria and selected water quality variables of the Missisquoi Bay were derived from Landsat ETM+ satellite image analyses in our previous study (Isenstein & Park 2014; Isenstein *et al.* 2014). A subset of variables for July (24th), August (9th) and September (11th) 2006 were analyzed. Water quality variables included cyanobacteria biovolume (Cyan), total nitrogen (TN), total phosphorus (TP), dissolved phosphorus (DP), particulate phosphorus (PP), the TN:TP ratio (by weight), Secchi depth (SD), and surface temperature (Temp). A bathymetry map (www.nauticalcharts.noaa.gov) and information on nutrient fluxes into Lake Champlain (USGS 2013) were provided as ancillary information. Contour plots of the difference in estimated concentrations of total phosphorus for both rivers (USGS 2013) were also employed.

Satellite-derived water quality images and ancillary information were managed with the GRASS GIS (grass.osgeo.org). All statistical analyses were developed with R software (www.r-project.com). A random pixel to a total of 10,000 was sampled for further statistical analysis. The locations of the sampled pixels were the same throughout the images. Annual time series of nutrient fluxes from the Missisquoi and Pike Rivers were transformed with the z-score to detect anomalies.

Exploratory analysis was conducted including descriptive statistics, removal of outliers, distribution assessment, and correlation analysis. Variables were not normally distributed based on the Kolmogorov–Smirnov test and therefore non-parametric methods were employed. Temporal differences of the studied variables were analyzed using the Kruskal–Wallis test. The Spearman rank correlation test was used to assess the relations of variables.

Regression analysis at each date was performed using generalized linear models (GLM) to relate the cyanobacteria biovolume with satellite-derived water quality variables as the GLM has been previously applied to predict phytoplankton distribution and environmental variables (Richardson *et al.* 2003; Demarcq *et al.* 2008; Williamson *et al.* 2010). The degree of multicollinearity among phosphorus variables showed that TP had the lowest variation inflation factor (VIF) and therefore was employed for further analyses. Then, five different models were developed to assess the influence of water quality variables on cyanobacteria: the first model included TP only; the second model included TN and TP; the third model added the SD to the second model; the fourth model added the Temp to the third model; and the fifth model included the TN:TP ratio, SD and Temp. Models were selected by their adjusted R-square, root mean square error (RMSE) and variance inflation factor (VIF). Selected models had VIF values lower than 5 (O'Brien 2007).

Geostatistical methods provided information on the spatial variability of cyanobacteria and selected predictive variables. The variogram analysis enabled the characterization of the underlying spatial process. The variogram provides a basis for interpreting the causes of the spatial variation and for identifying some of the controlling factors and processes (Webster & Oliver 2007). Nugget (C_0), sill (C), range (in m) and nugget:sill ratio ($C_0/C_0 + C$) were computed for that purpose. Theoretical variogram fitting was done with the gstat R-package (Pebesma 2004).

Spatial autocorrelation of cyanobacteria biovolume and the explanatory variables was assessed with the local indicators of spatial association (LISA) (Anselin 1995) for different distance-based weight matrices (i.e., 180 m, 250 m, 500 m and 1,000 m). The last three distances were selected based on the pixel size of moderate–coarse resolution satellite sensors (e.g., MODIS) in order to assess the clustering effect on the spatial autocorrelation of cyanobacteria and explanatory variables. This could provide valuable information about the up-scaling of Landsat-based water quality parameters to moderate–coarse resolution satellites for more frequent monitoring. Open GeoDa (geodacenter.asu.edu) software was employed for LISA analysis.

RESULTS AND DISCUSSION

Temporal significant differences were observed for both cyanobacteria and explanatory water quality variables during the summer of 2006 (Table 1).

A notable increase of cyanobacteria biovolume was observed, ranging from a median value of 80 mm^3/L in July to 206 mm^3/L in September, which are greater than the very-high-risk Alert Level 2 threshold (i.e., 10 mm^3/L) of the WHO (Bartram *et al.* 1999). TN slightly declined from a median value of 0.72 mg/L in July to below 0.6 mg/L in August and September. Phosphorus (i.e., total, particulate and dissolved) significantly increased from median TP values of below 60 μg/L in July and August to 77 μg/L in September. The TN:TP ratio slightly declined from a median value of 12.14 in July to 7.51 in September. SD also declined from a median value of 45 cm in August to 26 cm in September. The lake temperature declined from 297 K in July and August to 293 K in September.

Table 1 | Summary of descriptive statistics and Kruskal–Wallis test results for the selected satellite-derived water quality variables

Variables	Date	Median	Mean	St Dev	Min	Max	*p*-value
Cyanobacteria (mm^3/L)	Jul-2006	79.68	93.95	68.51	0.00	790.23	<0.001
	Aug-2006	100.09	106.30	66.50	0.00	790.98	
	Sep-2006	206.39	210.62	96.81	0.001	790.52	
Total nitrogen (mg/L)	Jul-2006	0.72	0.69	0.18	0.00	1.85	<0.001
	Aug-2006	0.59	0.58	0.13	0.002	1.11	
	Sep-2006	0.59	0.58	0.13	0.005	1.34	
Dissolved phosphorus (μg/L)	Jul-2006	28.54	28.85	9.13	0.00	266.48	<0.001
	Aug-2006	27.47	28.06	13.88	0.00	368.46	
	Sep-2006	37.59	37.40	16.51	0.00	319.05	
Particulate phosphorus (μg/L)	Jul-2006	22.27	22.85	7.79	0.00	109.73	<0.001
	Aug-2006	25.55	26.39	10.64	0.00	87.08	
	Sep-2006	42.09	41.84	15.17	0.00	190.58	
Total phosphorus (μg/L)	Jul-2006	58.88	59.71	18.04	0.00	283.83	<0.001
	Aug-2006	55.37	56.35	20.99	0.012	266.12	
	Sep-2006	76.73	75.75	28.17	0.00	401.22	
TN:TP	Jul-2006	12.14	12.31	3.88	0.05	64.95	<0.001
	Aug-2006	10.47	10.70	3.31	0.03	57.56	
	Sep-2006	7.51	7.69	2.20	0.12	59.38	
Secchi depth (cm)	Jul-2006	37.73	42.18	26.70	0.06	599.11	<0.001
	Aug-2006	44.59	53.16	44.58	4.18	608.56	
	Sep-2006	25.60	33.80	40.99	0.00	596.49	
Surface temperature (K)	Jul-2006	297.6	297.8	0.4	297.1	298.7	<0.001
	Aug-2006	297.1	297.1	0.4	296.0	298.2	
	Sep-2006	293.3	293.2	0.5	290.0	293.9	

The Spearman rank correlation test revealed some relations among cyanobacteria biovolume and explanatory variables (Table S-1, available with the online version of this paper): (1) positive high correlation (>0.7) with phosphorus variables; (2) negative high correlation (<−0.7) with Secchi depth; (3) moderate correlation with nitrogen; and (4) less evident inverse correlation with TN:TP ratio. As phosphorus has been reported as the major limiting nutrient of freshwater CyanoHABs (Paerl 2008), the correlation between cyanobacteria biovolume and phosphorus in Missisquoi Bay was evidence of the importance of P loadings in CyanoHABs development. This was also shown by the analysis of a time series of total annual yield of TP (Figure S-2, available online) (USGS 2013). High total annual yields of TP for Missisquoi and Pike Rivers in 2006 resulted from the streamflow conditions – above normal especially for July–September 2006 (http://water-watch.usgs.gov/) – that promoted transport of sediments and nutrients. The average temporal pattern (1994–2010) of TP revealed some seasonal differences in P loading from the two major rivers of the Missisquoi Bay (Figure S-3, available online). For the Missisquoi River, the variations in estimated TP concentrations were relatively evenly distributed throughout the year and the largest increases or decreases occurred at very high discharges (>95th percentile). The Pike River had a slight, fairly uniform decrease in concentrations of TP during most discharges and seasons, except for large increases at very high discharges in fall and winter. The different temporal pattern suggested that 2006 was a very wet year, leading to a massive input of phosphorus by runoff and subsequently to CyanoHAB events.

The most robust GLMs included TP, TN, SD and Temp (Table 2). GLM results implied the important influence of TN on CyanoHAB although the correlation between cyanobacteria biovolume and TN was rather moderate (Table S-2, available online). The *z*-score of the time series revealed anomalies in the N loadings into the Missisquoi Bay (Figure S-2) and nitrogen might also contribute to the cyanobacteria blooms. The better cyanobacteria prediction capabilities of the GLMs combining TP and TN agreed with previous studies at many freshwater lakes seriously affected by CyanoHABs, which revealed the need to control nitrogen loadings, along with phosphorus pollution (Paerl *et al.* 2011a; 2011b). Including SD, a proxy of turbidity, improved the predictive capabilities of GLMs. This agrees with the previous studies that CyanoHABs are associated with increased turbidity (Jacoby *et al.* 2000). Adding Temp also improved the performance of the GLMs as CyanoHABs are initiated and exacerbated with high surface water temperatures (>20 °C) (Paerl 1996), which were the case in the summer of 2006 in Missisquoi Bay. Thus, GLMs including the temperature as an explanatory variable (also including TN, TP and SD) reached better fitting results (R^2) and minimum errors.

Geostatistical analysis (Table 3) resulted in very similar theoretical variograms for cyanobacteria and total

Table 2 | Best performing generalized linear models of the prediction of cyanobacteria biovolume

	Fitting parameters			Values				
Model	R^2	**RMSE (mm³/L)**	**RMSE (%)**	**Variables**	**Estimate**	**Std Err**	***p*-value**	**VIF**
July	0.650	30.01	3.80	Intercept	−75.970	3.304	<0.001	
				TN	1.268	0.027	<0.001	1.198
				TP	0.008	0.001	<0.001	4.316
				SD	−0.510	0.015	<0.001	4.389
				Temp	0.268	0.011	<0.001	1.149
August	0.722	28.21	3.57	Intercept	−49.170	3.075	<0.001	
				TN	1.663	0.028	<0.001	1.170
				TP	0.003	0.000	<0.001	3.348
				SD	−0.443	0.008	<0.001	3.343
				Temp	0.179	0.010	<0.001	1.243
September	0.618	49.51	6.26	Intercept	24.052	2.329	<0.001	
				TN	1.002	0.030	<0.001	1.297
				TP	−0.001	0.000	<0.001	2.256
				SD	−0.602	0.010	<0.001	2.093
				Temp	−0.064	0.008	<0.001	1.049

phosphorus. The range closely evolved along time for both parameters (Figure S-4, available online). It suggest similar spatial dependence limits (correlation range) and spatial autocorrelation. Besides, a notable increase of the range from July to August for all variables was shown. The nugget:sill ratio was moderate although slightly increased with the HAB event. It suggests a mild local noise in the spatial variables.

The LISA Moran's I results showed moderate positive autocorrelations with phosphorus variables while the other variables did not exhibit autocorrelation (Table 4), as higher positive values indicate a stronger direct relationship between cyanobacteria biovolume and explanatory variables. The trend of TP was the progressive reduction of spatial autocorrelation as the weight distance increased. These observations suggested a structured spatial relationship between cyanobacteria and TP at the multiple scales of the study.

The LISA test resulted in significance and cluster maps between cyanobacteria and phosphorus (Figure 1). These maps illustrate the spatial and temporal evolution of the relationship between cyanobacteria and TP at 250 m of spatial lag. This spatial resolution was selected because it is the highest resolution of high-time frequency moderate spatial resolution sensors like MODIS. These types of sensors have lower spatial resolution but frequent revisiting-time (i.e. 1–3 days) and therefore they are highly valuable for Cyano-HAB monitoring (Matthews *et al.* 2010; Odermatt *et al.* 2012; Wheeler *et al.* 2012) while Landsat provides higher spatial resolution (30 m) but limited revisiting time (i.e. 16 days). The comparability of results for both types of sensors in aquatic ecosystems has been dealt with by accounting the spatial autocorrelation processes (Melendez-Pastor *et al.* 2010). Significance maps denote points of a statistically significant correlation between cyanobacteria and TP (green points). The displacement of significance points patches was evident throughout the study period. This observation suggested movements of nutrients and cyanobacteria within Missisquoi Bay by winds and water fluxes (Qin *et al.* 2010; Bresciani *et al.* 2013).

The cluster maps (Figure 1) provide the location of high correlation patches between cyanobacteria and TP within Missisquoi Bay. Dark red points denote 'hot-spots' of high cyanobacteria biovolume and high TP concentrations while dark blue points denote areas with low cyanobacteria biovolume and low TP concentrations. Very large patches of high–high correlation were observed over the deepest areas of the Bay (see Figure S-1, bathymetry map), especially in July and August. Hence, a potential influence of water depth in the initiation of the bloom could be expected as the bloom can be affected by the morphology of the water body, e.g. the water depth representing the thickness of the stratum (Chorus & Cavalieri 2000). Previous remote sensing studies reported the temporal variation of high concentrations of phytoplankton at various depths, with growth as a result of stratification during the summer (Odermatt *et al.* 2012). This phenomenon along with the wind and

Table 3 | Theoretical variogram fitting parameters

Variables	Date	Model	Nugget (C_0)	Sill (C)	Range (in m)	$C_0/(C_0+C)$
Cyanobacteria (mm^3/L)	Jul-2006	Spherical	226.1	2,151	2,959	0.10
	Aug-2006	Spherical	368.3	1,979	5,492	0.16
	Sep-2006	Spherical	823.2	5,559	5,325	0.13
Total nitrogen (mg/L)	Jul-2006	Exponential	0.003	0.018	1,662	0.16
	Aug-2006	Exponential	0.004	0.006	1,451	0.39
	Sep-2006	Exponential	0.005	0.006	1,693	0.44
Total phosphorus (μg/L)	Jul-2006	Spherical	28.10	199.3	2,821	0.12
	Aug-2006	Spherical	28.77	269.9	5,785	0.10
	Sep-2006	Spherical	60.60	231.3	4,266	0.21
Secchi depth (cm)	Jul-2006	Circular	0.018	0.308	2,369	0.06
	Aug-2006	Circular	0.039	0.379	5,411	0.09
	Sep-2006	Exponential	0.016	0.129	2,489	0.11
Surface temperature (K)	Jul-2006	Exponential	0.010	0.081	3,708	0.11
	Aug-2006	Spherical	0.010	0.029	5,163	0.26
	Sep-2006	Exponential	0.008	0.039	2,315	0.18

Table 4 | LISA Moran's I for cyanobacteria vs selected variables for coincident dates (500 iterations)

		Weight distance			
Variables	Date	180	250	500	1,000
TN	TN Jul-2006	0.0570	0.0308	−0.0068	−0.0112
	TN Aug-2006	0.0001	−0.0089	−0.0326	−0.0348
	TN Sep-2006	−0.0305	−0.0336	−0.0363	−0.0290
TP	TP Jul-2006	0.4086	0.3838	0.3152	0.2244
	TP Aug-2006	0.4483	0.4444	0.4164	0.3612
	TP Sep-2006	0.3417	0.3073	0.2366	0.1747
SD	SD Jul-2006	−0.1948	−0.1857	−0.1577	−0.1128
	SD Aug-2006	−0.0357	−0.0408	−0.0356	−0.0318
	SD Sep-2006	−0.0239	−0.0242	−0.0175	−0.0083
Temp	ST Jul-2006	0.1445	0.1289	0.0940	0.0570
	ST Aug-2006	0.0257	0.0229	0.0163	0.0109
	ST Sep-2006	0.0867	0.0686	0.0409	0.0285

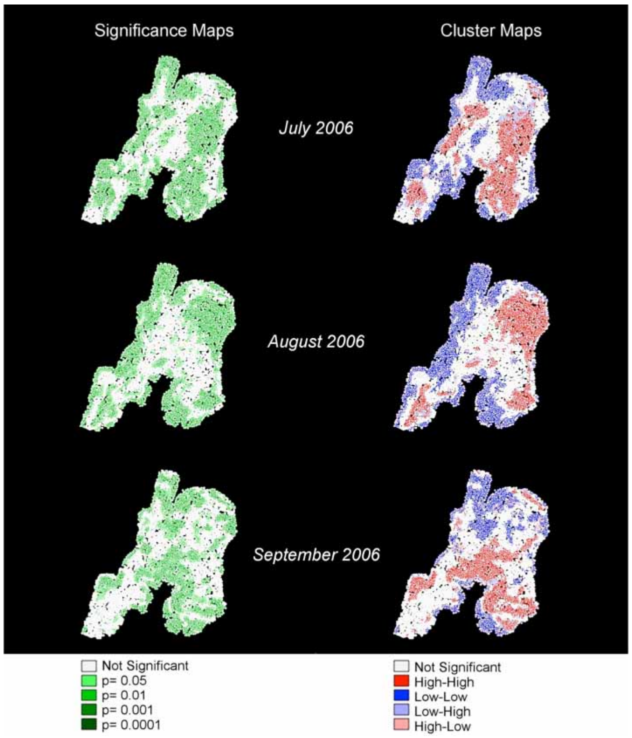

Figure 1 | Temporal evolution of the significance and cluster maps from the LISA test of cyanobacteria vs TP.

water currents could explain the temporal displacement of the high–high correlation of cyanobacteria and TP in Missisquoi Bay, from the deepest areas in early summer to the southern shallower areas in late summer.

CONCLUSIONS

Missisquoi Bay is a eutrophic, prone to CyanoHAB development portion of Lake Champlain. Satellite remote sensing has been previously employed to predict cyanobacteria blooms. The spatial–temporal influence of nutrient levels, turbidity and temperature on cyanobacteria blooms require further attention. This study employed satellite-derived cyanobacteria and explanatory water quality variables to assess the spatial–temporal dynamic of a bloom event in the summer of 2006 in Missisquoi Bay. The influence of nutrient loadings and hydrological conditions as the driving forces of the bloom event was found. Cyanobacteria biovolume was highly correlated with phosphorus and turbidity during the summer. Heavy rainfall promoted the entrainment of large amounts of nutrients and sediments through the rivers that drain into the Bay. The influence of nitrogen and temperature in the bloom event was shown by the results of GLMs of cyanobacteria blooms. Thus, nutrient and non-nutrient explanatory variables synergistically interacted to promote a bloom event with extreme climate and hydrological conditions. The multi-scale autocorrelation between cyanobacteria and TP was revealed with the variogram analysis and the LISA test, which showed a complex dynamic and displacement from deepest-to-shallowest areas of high correlations between both variables throughout the summer. The autocorrelation among cyanobacteria and TP was maintained at multiple resolutions thus suggesting the possibility of up-scaling the current results to coarse resolution satellite imagery for more frequent monitoring of bloom events.

REFERENCES

Agha, R., Cirés, S., Wörmer, L., Domínguez, J. A. & Quesada, A. 2012 Multi-scale strategies for the monitoring of freshwater cyanobacteria: reducing the sources of uncertainty. *Water Research* **46**, 3043–3053.

Anderson, D. M., Glibert, P. M. & Burkholder, J. M. 2002 Harmful algal blooms and eutrophication: nutrient sources, composition, and consequences. *Estuaries* **25** (4), 704–726.

Anselin, L. 1995 Local indicators of spatial association – LISA. *Geographical Analysis* **27** (2), 93–115.

Bartram, J., Burch, M., Falconer, I. R., Jones, G. & Kuiper-Goodman, T. 1999 Situation assessment, planning and management. In: *Toxic Cyanobacteria in Water: A Guide to Their Public Health Consequences, Monitoring and Management* (I. Chorus & J. Bartram, eds), World Health Organization (WHO), London and New York, pp. 183–210.

Bowling, L. C., Blais, S. & Sinotte, M. 2015 Heterogeneous spatial and temporal cyanobacterial distributions in Missisquoi Bay, Lake Champlain: an analysis of a 9 year data set. *Journal of Great Lakes Research* **41** (1), 164–179.

Boyer, G. L. 2008 Cyanobacterial toxins in New York and the lower Great Lakes ecosystems. In: *Cyanobacterial Harmful Algal Blooms: State of the Science and Research Needs* (H. K. Hudnell, ed.), Springer Science + Business Media, New York, USA, pp. 153–165.

Bresciani, M., Adamo, M., De Carolis, G., Matta, E., Pasquariello, G., Vaičiūtė, D. & Giardino, C. 2013 Monitoring blooms and surface accumulation of cyanobacteria in the Curonian Lagoon by combining MERIS and ASAR data. *Remote Sensing of Environment* **146**, 124–135.

Chorus, I. & Cavalieri, M. 2000 Cyanobacteria and algae. In: *Monitoring Bathing Waters – A Practical Guide to the Design and Implementation of Assessments and Monitoring Programmes* (J. Bartram & G. Rees, eds), World Health Organization (WHO), London and New York, pp. 205–258.

Demarcq, H., Richardson, A. J. & Field, J. G. 2008 Generalised model of primary production in the southern Benguela upwelling system. *Marine Ecology Progress Series* **354**, 59–74.

Isenstein, E. M. & Park, M.-H. 2014 Assessment of nutrient distributions in Lake Champlain using satellite remote sensing. *Journal of Environmental Sciences* **26** (9), 1831–1836.

Isenstein, E. M., Trescott, A. & Park, M.-H. 2014 Multispectral remote sensing of harmful algal blooms in Lake Champlain, USA. *Water Environment Research* **86** (12), 2271–2278.

Jacoby, J. M., Collier, D. C., Welch, E. B., Hardy, F. J. & Crayton, M. 2000 Environmental factors associated with a toxic bloom of *Microcystis aeruginosa*. *Canadian Journal of Fisheries and Aquatic Sciences* **57** (1), 231–240.

Kutser, T., Metsamaa, L., Strömbeck, N. & Vahtmäe, E. 2006 Monitoring cyanobacterial blooms by satellite remote sensing. *Estuarine, Coastal and Shelf Science* **67**, 303–312.

Levine, S. N., Lini, A., Ostrofsky, M. L., Bunting, L., Burgess, H., Leavitt, P. R., Reuter, D., Lami, A., Guilizzoni, P. & Gilles, E. 2012 The eutrophication of Lake Champlain's northeastern arm: insights from paleolimnological analyses. *Journal of Great Lakes Research* **38** (Supplement 1), 35–48.

Matthews, M. W., Bernard, S. & Winter, K. 2010 Remote sensing of cyanobacteria-dominant algal blooms and water quality parameters in Zeekoevlei, a small hypertrophic lake, using MERIS. *Remote Sensing of Environment* **114**, 2070–2087.

Melendez-Pastor, I., Navarro-Pedreño, J., Koch, M. & Gómez, I. 2010 Multi-resolution and temporal characterization of land use classes in a Mediterranean wetland with land cover fractions. *International Journal of Remote Sensing* **31** (20), 5365–5389.

O'Brien, R. M. 2007 A caution regarding rules of thumb for variance inflation factors. *Quality & Quantity* **41** (5), 673–690.

Odermatt, D., Pomati, F., Pitarch, J., Carpenter, J., Kawka, M., Schaepman, M. & Wüest, A. 2012 MERIS observations of phytoplankton blooms in a stratified eutrophic lake. *Remote Sensing of Environment* **126**, 232–239.

Paerl, H. W. 1996 A comparison of cyanobacterial bloom dynamics in freshwater, estuarine and marine environments. *Phycologia* **35** (6S), 25–35.

Paerl, H. 2008 Nutrient and other environmental controls of harmful cyanobacterial blooms along the freshwater–marine continuum. In: *Cyanobacterial Harmful Algal Blooms: State of the Science and Research Needs* (H. K. Hudnell, ed.), Springer Science + Business Media, New York, USA, pp. 217–237.

Paerl, H. W. & Huisman, J. 2009 Climate change: a catalyst for global expansion of harmful cyanobacterial blooms. *Environmental Microbiology Reports* **1** (1), 27–37.

Paerl, H. W., Hall, N. S. & Calandrino, E. S. 2011a Controlling harmful cyanobacterial blooms in a world experiencing anthropogenic and climatic-induced change. *Science of the Total Environment* **409** (10), 1739–1745.

Paerl, H. W., Xu, H., McCarthy, M. J., Zhu, G., Qin, B., Li, Y. & Gardner, W. S. 2011b Controlling harmful cyanobacterial blooms in a hyper-eutrophic lake (Lake Taihu, China): the need for a dual nutrient (N & P) management strategy. *Water Research* **45** (5), 1973–1983.

Pebesma, E. J. 2004 Multivariable geostatistics in S: the gstat package. *Computers & Geosciences* **30**, 683–691.

Qin, B., Zhu, G., Gao, G., Zhang, Y., Li, W., Paerl, H. W. & Carmichael, W. W. 2010 A drinking water crisis in Lake Taihu, China: linkage to climatic variability and lake management. *Environmental Management* **45** (1), 105–112.

Richardson, A. J., Silulwane, N. F., Mitchell-Innes, B. A. & Shillington, F. A. 2003 A dynamic quantitative approach for predicting the shape of phytoplankton profiles in the ocean. *Progress in Oceanography* **59**, 301–319.

USGS 2013 *Concentration, Flux, and the Analysis of Trends of Total and Dissolved Phosphorus, Total Nitrogen, and Chloride in 18 Tributaries to Lake Champlain, Vermont and New York, 1990–2011*. Report US Geological Survey (USGS), Reston, VA, USA.

Webster, R. & Oliver, M. A. 2007 *Geostatistics for Environmental Scientists*, 2nd edn. John Wiley & Sons Ltd, Chichester, UK.

Wheeler, S. M., Morrissey, L. A., Levine, S. N., Livingston, G. P. & Vincent, W. F. 2012 Mapping cyanobacterial blooms in Lake Champlain's Missisquoi Bay using QuickBird and MERIS satellite data. *Journal of Great Lakes Research* **38**, 68–75.

Williamson, R., Field, J. G., Shillington, F. A., Jarre, A. & Potgieter, A. 2010 A Bayesian approach for estimating vertical chlorophyll profiles from satellite remote sensing: proof-of-concept. *ICES Journal of Marine Science* **68**, 792–799.

First received 20 July 2018; accepted in revised form 10 January 2019. Available online 24 January 2019

SUPPLEMENTARY MATERIAL

Table S-1 Spearman rank correlation matrix of satellite-derived water quality variables. High correlations (>0.7 or <-0.7) are highlighted in bold and moderate correlations (>0.5 or <-0.5) are in italics.

		Cyanobacteria			TN			TP			DP			PP			TN:TP			Secchi disk			Temperature		
		Jul	Aug	Sep	Jul	Aug	Sep	Jul	Aug	Sep	Jul	Aug	Sep	Jul	Aug	Sep	Jul	Aug	Sep	Jul	Aug	Sep	Jul	Aug	Sep
Cyan	Jul	1																							
	Aug	0.08	1																						
	Sep	0.11	0.13	1																					
TN	Jul	0.36	-0.25	0.16	1																				
	Aug	0.10	0.38	-0.03	0.01	1																			
	Sep	0.13	-0.02	0.44	0.18	0.11	1																		
TP	Jul	**0.72**	0.15	0.11	0.18	0.06	0.09	1																	
	Aug	0.04	**0.76**	0.12	-0.31	0.12	-0.05	0.12	1																
	Sep	0.09	0.09	**0.71**	0.14	-0.09	0.25	0.12	0.11	1															
DP	Jul	**0.79**	0.13	0.13	0.38	0.08	0.12	**0.92**	0.09	0.13	1														
	Aug	0.07	**0.81**	0.14	-0.31	0.33	-0.02	0.14	**0.94**	0.12	0.11	1													
	Sep	0.11	0.12	**0.77**	0.15	-0.06	*0.50*	0.14	0.14	**0.91**	0.15	0.15	1												
PP	Jul	**0.72**	0.26	0.12	-0.03	0.06	0.05	**0.94**	0.25	0.12	**0.88**	0.27	0.13	1											
	Aug	0.07	**0.76**	0.16	-0.34	0.07	-0.04	0.16	**0.97**	0.15	0.13	**0.94**	0.18	0.31	1										
	Sep	0.09	0.13	**0.72**	0.10	-0.12	0.19	0.14	0.16	**0.97**	0.14	0.17	**0.91**	0.15	0.22	1									
TN:TP	Jul	-0.37	-0.31	0.00	*0.50*	-0.01	0.08	**-0.71**	-0.33	-0.03	*-0.50*	-0.34	-0.02	**-0.81**	-0.38	-0.08	1								
	Aug	0.04	-0.46	-0.10	0.33	0.41	0.14	-0.07	**-0.80**	-0.15	-0.02	*-0.62*	-0.14	-0.19	**-0.81**	-0.21	0.32	1							
	Sep	0.02	-0.07	-0.28	0.03	0.18	0.49	-0.04	-0.13	*-0.64*	-0.02	-0.12	-0.39	-0.06	-0.17	*-0.67*	0.10	0.25	1						
SD	Jul	**-0.74**	-0.03	-0.06	-0.27	0.00	-0.07	**-0.93**	0.01	-0.10	**-0.89**	0.00	-0.09	**-0.85**	-0.02	-0.11	*0.60*	-0.01	0.03	1					
	Aug	-0.04	**-0.76**	-0.08	0.33	-0.15	0.07	-0.11	**-0.98**	-0.08	-0.08	**-0.94**	-0.10	-0.24	**-0.96**	-0.14	0.34	**0.78**	0.12	0.01	1				
	Sep	-0.09	-0.07	**-0.75**	-0.14	0.10	-0.24	-0.12	-0.10	**-0.96**	-0.13	-0.11	**-0.89**	-0.11	-0.14	**-0.95**	0.03	0.15	*0.64*	0.10	0.07	1			
Temp	Jul	0.10	0.29	-0.09	-0.36	0.23	-0.03	0.10	0.28	-0.11	0.08	0.30	-0.10	0.21	0.26	-0.10	-0.31	-0.15	0.08	-0.01	-0.29	0.11	1		
	Aug	-0.01	0.40	0.11	-0.26	0.06	-0.04	0.06	0.44	0.08	0.02	0.44	0.09	0.15	0.45	0.12	-0.25	-0.38	-0.10	0.04	-0.42	-0.09	0.23	1	
	Sep	0.06	0.22	0.00	0.01	0.16	0.08	0.08	0.21	0.02	0.10	0.20	0.04	0.06	0.18	0.02	-0.03	-0.10	0.07	-0.07	-0.21	0.05	0.10	0.10	1

Table S-2 Generalized linear models results of the prediction of cyanobacteria biovolume from explanatory variables.

Date	Model	Fitting parameters			Values				
		R^2	RMSE (mm^3/L)	RMSE (%)	Variables	Estimate	Std Err	*p*-value	VIF
July	J1	0.167	62.23	8.00	Intercept	3.872	0.031	<0.001	
					TP	0.011	0.001	<0.001	
	J2	0.433	42.34	5.36	Intercept	2.596	0.035	<0.001	
					TN	1.281	0.039	<0.001	1.016
					TP	0.016	0.000	<0.001	1.016
	J3	0.004	57.66	7.30	Intercept	4.835	0.052	<0.001	
					TN	-0.468	0.030	<0.001	1.051
					TP	0.003	0.000	<0.001	2.494
					SD	-0.032	0.014	0.017	2.571
	J4	0.650	30.01	3.80	Intercept	-75.970	3.304	<0.001	
					TN	1.268	0.027	<0.001	1.198
					TP	0.008	0.001	<0.001	4.316
					SD	-0.510	0.015	<0.001	4.389
					Temp	0.268	0.011	<0.001	1.149
	J5	0.588	31.11	3.94	Intercept	-67.363	3.574	<0.001	
					TN:TP	0.047	0.002	<0.001	1.869
					SD	-0.975	0.010	<0.001	1.691
					Temp	0.245	0.012	<0.001	1.165
August	A1	0.252	58.48	7.39	Intercept	4.096	0.024	<0.001	
					TP	0.010	0.000	<0.001	
	A2	0.535	56.65	7.16	Intercept	2.428	0.018	<0.001	
					TN	1.759	0.030	<0.001	1.120
					TP	0.019	0.000	<0.001	1.120
	A3	0.712	28.79	3.64	Intercept	4.094	0.035	<0.001	
					TN	1.612	0.028	<0.001	1.169
					TP	0.004	0.000	0.006	3.158
					SD	-0.458	0.008	<0.001	3.294
	A4	0.722	28.21	3.57	Intercept	-49.170	3.075	<0.001	
					TN	1.663	0.028	<0.001	1.170
					TP	0.003	0.000	<0.001	3.348
					SD	-0.443	0.008	<0.001	3.343
					Temp	0.179	0.010	<0.001	1.243

Date	Model	Fitting parameters			Values				
		R^2	RMSE (mm³/L)	RMSE (%)	Variables	Estimate	Std Err	*p*-value	VIF
	A5	0.690	27.31	3.45	Intercept	-50.698	3.340	<0.001	
					TN:TP	0.0049	0.001	<0.001	1.912
					SD	-0.700	0.007	<0.001	1.945
					Temp	0.188	0.011	<0.001	1.201
September	S1	0.167	88.37	11.18	Intercept	4.907	0.006	<0.001	
					TP	0.016	0.000	<0.001	
	S2	0.261	84.40	10.68	Intercept	4.272	0.020	<0.001	
					TN	0.881	0.035	<0.001	1.201
					TP	0.007	0.000	<0.001	1.201
	S3	0.603	51.38	6.50	Intercept	5.418	0.028	<0.001	
					TN	0.957	0.030	<0.001	1.217
					TP	-0.001	0.000	<0.001	2.132
					SD	-0.609	0.010	<0.001	2.041
	S4	0.618	49.51	6.26	Intercept	24.052	2.329	<0.001	
					TN	1.002	0.030	<0.001	1.297
					TP	-0.001	0.000	<0.001	2.256
					SD	-0.602	0.010	<0.001	2.093
					Temp	-0.064	0.008	<0.001	1.049
	S5	0.617	45.09	5.70	Intercept	5.328	2.083	0.018	
					TN:TP	0.044	0.001	<0.001	1.281
					SD	-0.801	0.007	<0.001	1.285
					Temp	0.001	0.007	0.881	1.004

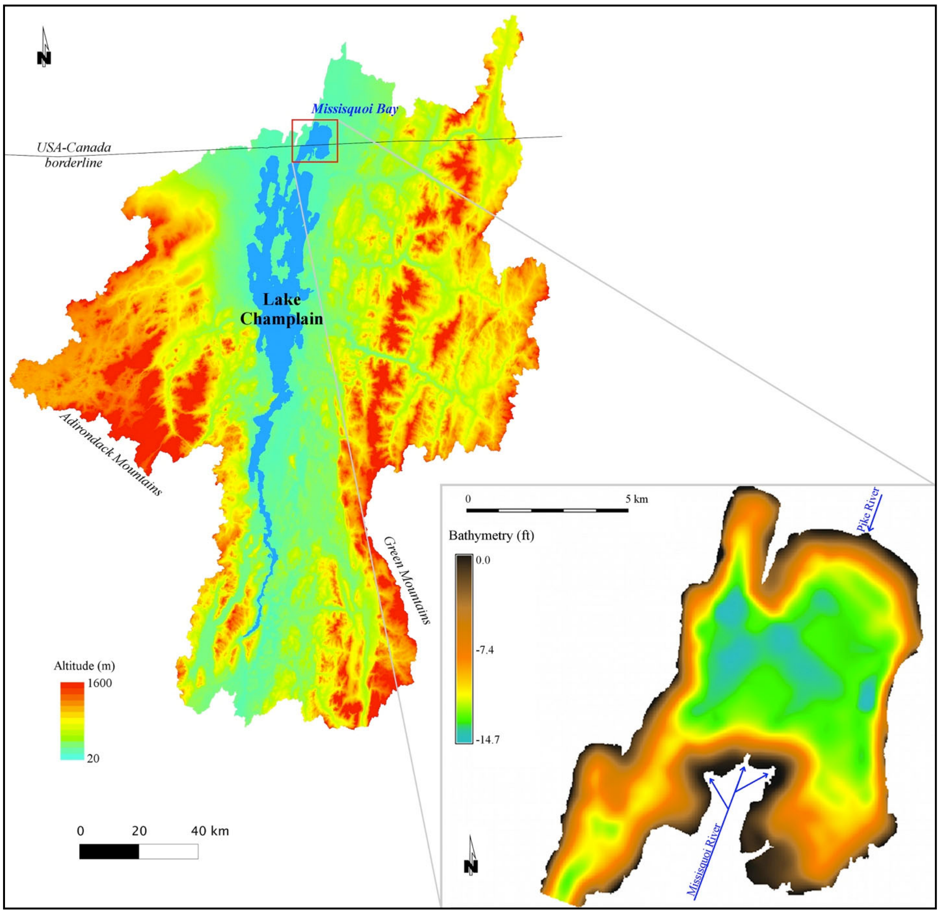

Figure S-1 Location of the Missisquoi Bay in the Lake Champlain basin and bathymetry of the study area.
Digital elevation model provided by the US Geological Survey.

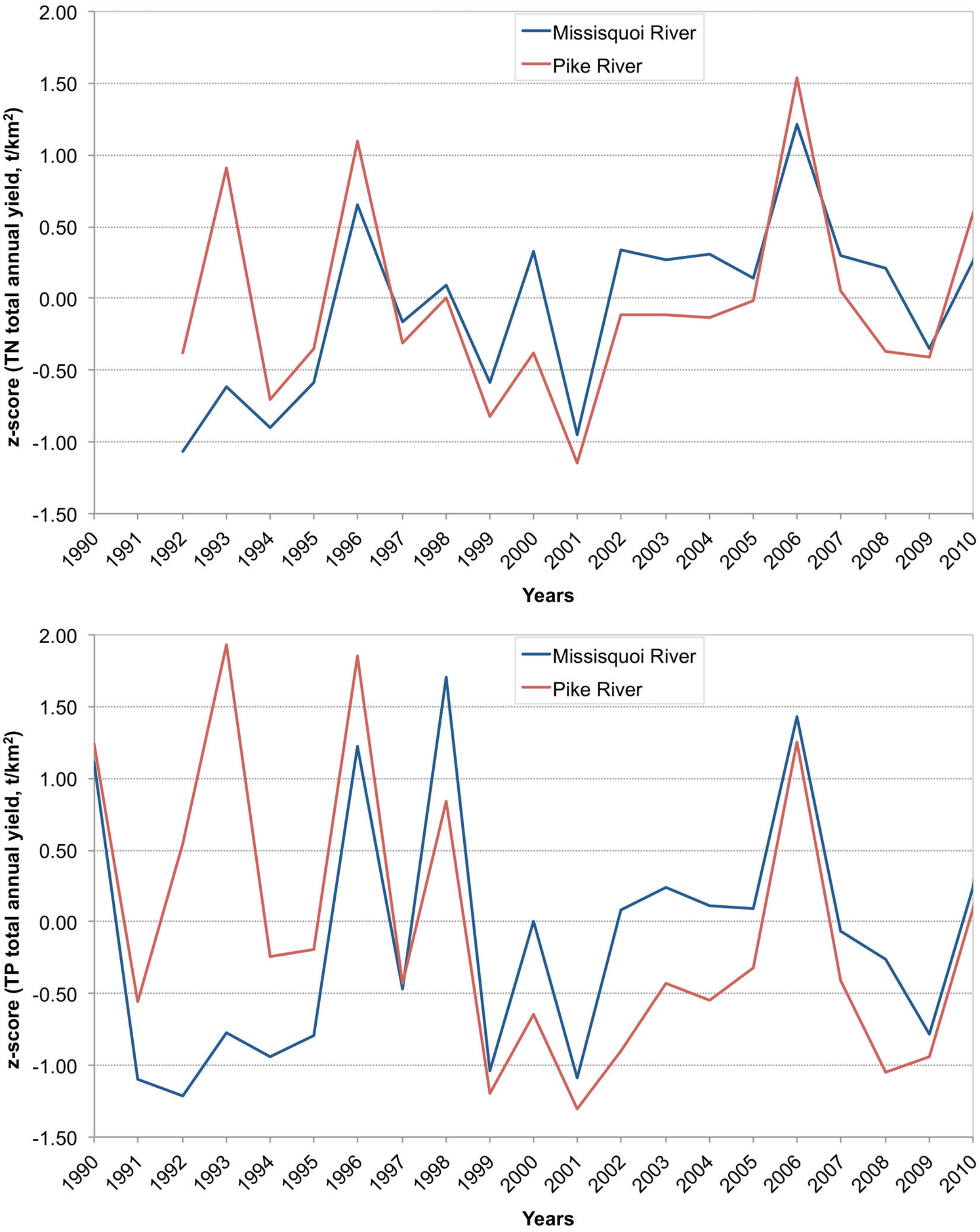

Figure S-2 *Z*-score of the time series (1990–2010) of total annual yield of total nitrogen (upper) and total phosphorus (lower) for Missisquoi and Pike Rivers. Original data from USGS, 2013.

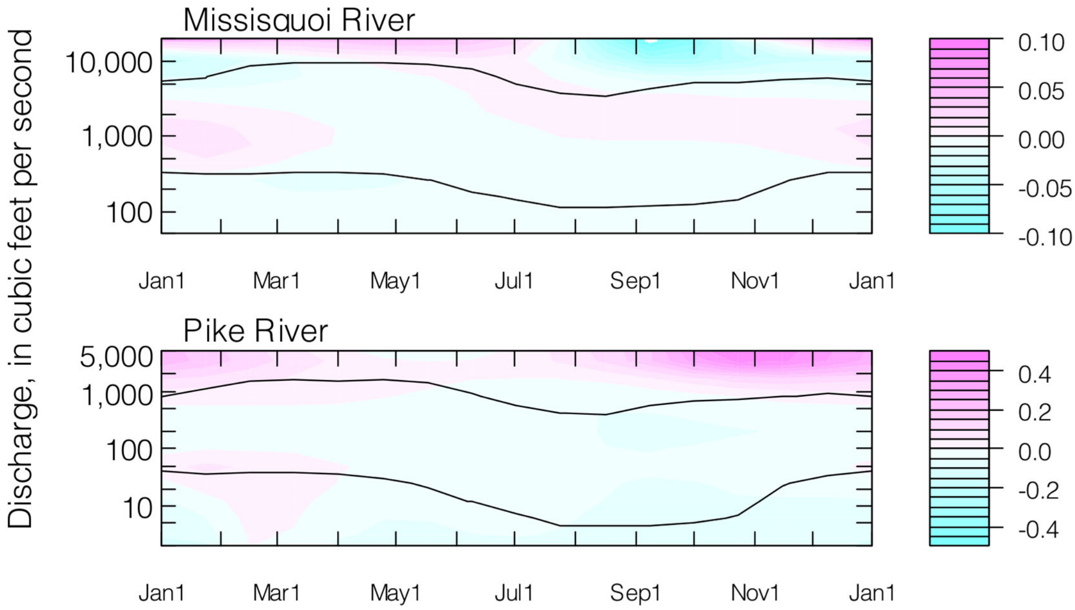

Figure S-3 Contour plots of the difference in estimated concentrations of total phosphorus for Missisquoi and Pike Rivers for the time series (1994-2010). Color ramp represents difference in concentration, in mg/L. Source: USGS, 2013.

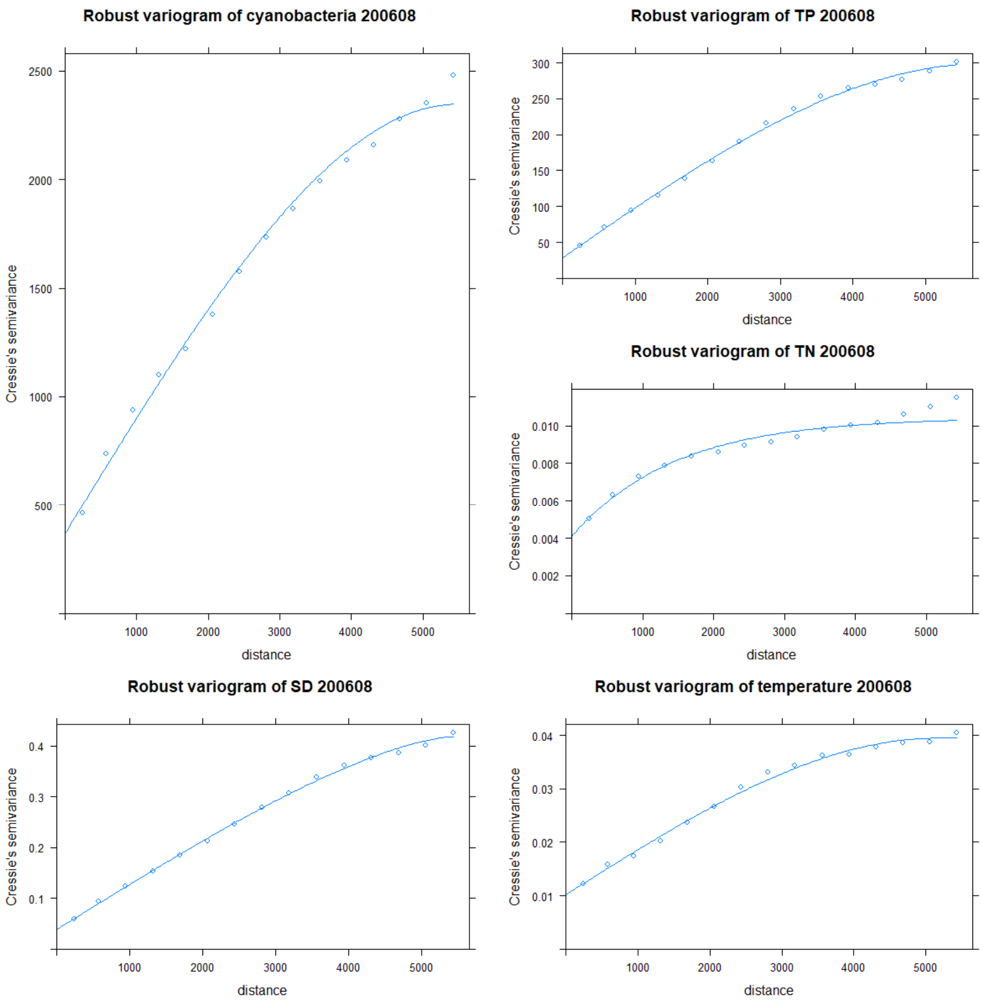

Figure S-4 Fitted variogram for the cyanobacteria and predictive variables in August.